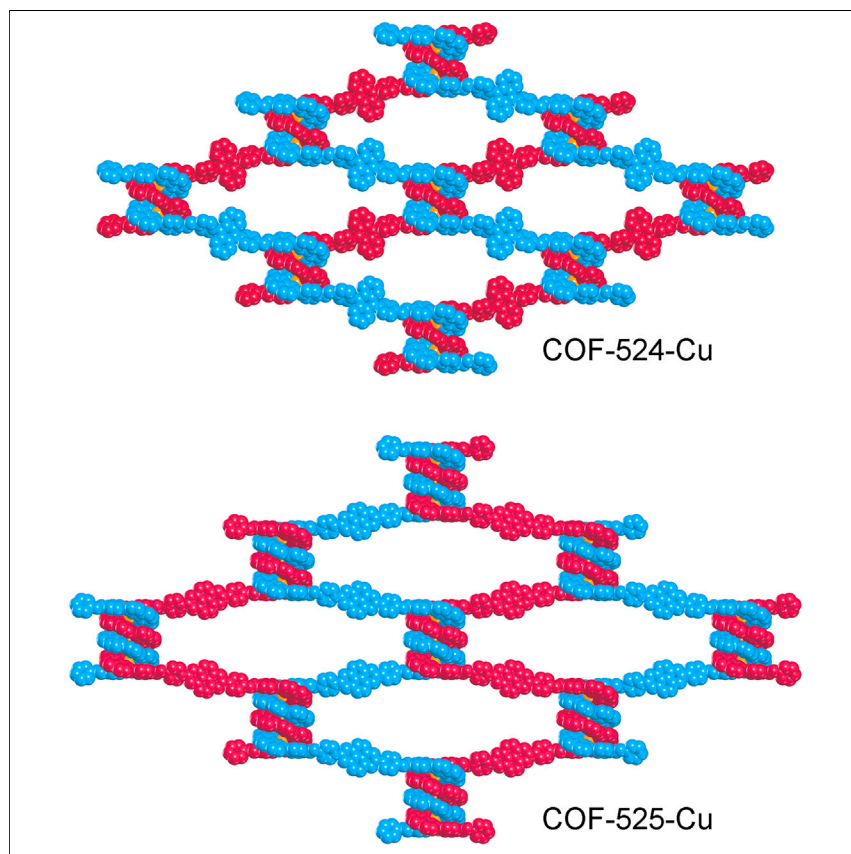


Article

Molecular weaving of chicken-wire covalent organic frameworks



Preparing woven 2D structures of COFs is challenging. In this study, Yaghi and co-workers use helicates composed of multiple mutually embracing complexes to access the planar building units necessary for making 2D patterns. They achieve two distinct chicken-wire patterns by controlling the number of turns in these helical building units.

Xing Han, Tianqiong Ma, Brent L. Nannenga, ..., Robert O. Ritchie, Yong Cui, Omar M. Yaghi

yongcui@sjtu.edu.cn (Y.C.)
yaghi@berkeley.edu (O.M.Y.)

Highlights

Design and synthesis of molecular chicken wire via COF chemistry

The number of turns and the crossing points direct how the threads are woven in the COFs

A new approach for achieving 2D woven COFs by installing functionalized polynuclear helicates

Article

Molecular weaving of chicken-wire covalent organic frameworks

Xing Han,^{1,2,10} Tianqiong Ma,^{1,2} Brent L. Nannenga,^{3,4} Xuan Yao,⁵ S. Ephraim Neumann,^{1,2} Punit Kumar,^{6,7} Junpyo Kwon,^{6,7} Zichao Rong,^{1,2} Kaiyu Wang,^{1,2} Yuebiao Zhang,⁵ Jorge A.R. Navarro,⁹ Robert O. Ritchie,^{6,7,8} Yong Cui,^{10,*} and Omar M. Yaghi^{1,2,11,*}

SUMMARY

Molecular weaving is the interlacing of covalently linked threads to make extended structures. Although weaving based on 3D networks has been reported, the 2D forms remain largely unexplored. Reticular chemistry uses mutually embracing tetrahedral metal complexes as crossing points, which, when linked, typically lead to 3D woven structures. Realizing 2D weaving patterns requires crossing points with an overall planar geometry. We show that polynuclear helicates composed of multiple metal-complex units, and therefore multiple turns, are well suited in this regard. By reticulating helicate units, we successfully obtained 2D weaving structures based on the familiar chicken-wire pattern.

INTRODUCTION

The power of reticular chemistry has been illustrated in making metal-organic frameworks (MOFs) and covalent organic frameworks (COFs) with predetermined structures.¹ Recently, molecular weaving has further expanded this chemistry by using either weak intermolecular forces or mutually embracing metal complexes to create woven structures wherein long threads are interlaced.^{2–8} Previous work has employed such complexes with an overall tetrahedral geometry to consistently give 3D woven and interlocked frameworks.^{5–8} In our attempt to expand the scope of this chemistry, we asked the question of how one maintains the necessity of having mutually embracing complexes for weaving to take place while targeting topologies other than 3D networks. Namely, how do we prepare woven 2D structures? We believe that such arrangements are of fundamental importance to achieving properties, which make woven fabric and metal fences so pervasive in our society. In this work, we show how helicates^{9–12} composed of multiple mutually embracing complexes can indeed be used for accessing the very planar building units necessary for making 2D patterns (Figures S1 and S2). By controlling the number of turns in these helical building units, we achieve two distinct chicken-wire patterns (Figure 1).

The key to designing new molecular weaving patterns is to choose a mutually embracing metal complex, which serves as a crossing point. The linking groups (points of extension) define its overall geometry, and in reticulating an extended woven structure there are three factors to be considered: (1) the angles between these geometric units determine the dimensionality of the woven pattern, (2) the directionality of the points of extension control the propagation of the structure, and (3) the relative orientation of the units bearing the points of extension will ultimately determine the type of pattern. The last factor is especially useful for helicates because of their chirality: an aspect typically not considered in MOF or COF

THE BIGGER PICTURE

Helical building units were used in the synthesis of molecular chicken wires. The creation of such 2D patterns, the most prevalent macroscopic type of weaving in society, has been uncommon. In this work, we demonstrate that helically assembled molecules, helicates, composed of multiple mutually embracing complexes, can indeed be used for accessing the planar building units necessary for making 2D woven patterns. By controlling the number of turns in these helical building units, we can generate two distinct patterns that resemble chicken-wire fences. We believe that such arrangements are of fundamental importance for venturing further into achieving properties that make woven fabric and metal fences so ubiquitous in our society.

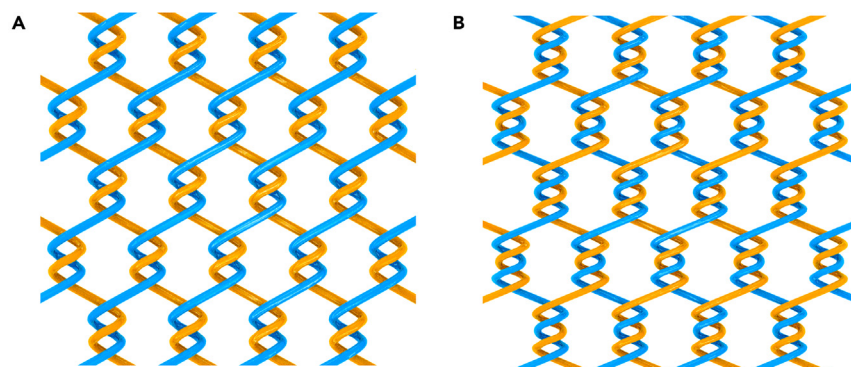


Figure 1. Illustrations of woven threads in two dimensions

2D woven patterns constructed from helical building units with (A) two and (B) three turns.

construction but essential to molecular weaving by design. In our pursuit of 2D weaving, we use two- and three-turn helicates to illustrate how two patterns can be achieved, where the threads propagate either orthogonally or parallel to each other (Figure 1). Our synthetic strategy is shown in Figure 2. The weaving nodes dicopper(I)-bis{4,4'-(1,3-phenylenebis(1,10-phenanthroline-9,2-diyl))dibenzaldehyde} tetrafluoroborate ($\text{Cu}_2(\text{PPD})_2(\text{BF}_4)_2$) and tricopper-bis{2,9-bis[3-(9-(4-(dimethoxymethyl)phenyl)-1,10-phenanthroline-2-yl)phenyl]-1,10-phenanthroline}tritetrafluoroborate ($\text{Cu}_3(\text{DPPP})_2(\text{BF}_4)_3$) can be functionalized with either aldehyde or dimethoxymethyl groups. The functional groups can be linked with 9,10-bis(4-aminophenyl)anthracene (BAA) or 2,7-bis(4-aminophenyl)pyrene (BAP) to make an imine-bonded PPD-BAA or DPPP-BAP thread, respectively. These two complexes include two or three copper(I) ions and have been studied extensively as discrete molecules for the formation of molecular knots.^{13,14} The single-crystal structures of the complexes and their analogs confirm a pseudo-planar geometry at the helicate edges (Figures S1 and S2), which ensures the assembly of the threads into a 2D framework, resembling a chicken wire. Mechanical measurements by nanoindentation indicate that upon removal of the Cu(I) ions, the threads become solely held together by mechanical bonds, thereby making the material even more elastic.

RESULTS AND DISCUSSION

Synthesis and characterization

The synthesis of COF-524-Cu ($[\text{Cu}_2(\text{PPD})_2(\text{BF}_4)_2(\text{BAA})_2]_{\text{imine}}$) or COF-525-Cu ($[\text{Cu}_3(\text{DPPP})_2(\text{BF}_4)_3(\text{BAP})_2]_{\text{imine}}$) was carried out with equimolar amounts of $\text{Cu}_2(\text{PPD})_2(\text{BF}_4)_2$ or $\text{Cu}_3(\text{DPPP})_2(\text{BF}_4)_3$, respectively, and BAA or BAP, respectively, which were reacted in dioxane or a 1:3 (v/v) mixture of *N,N*-dimethylacetamide (DMA) and chlorobenzene (CB) in the presence of aqueous acetic acid as a catalyst. The reaction mixture was sealed in a Pyrex tube and heated at 120°C. After 7 days, the resulting precipitate was collected and washed by Soxhlet extraction with anhydrous tetrahydrofuran to yield a dark-brown crystalline solid, which was found to be insoluble in common organic solvents and water. The formation of imine linkages in the COFs was confirmed by Fourier-transform infrared (FT-IR) spectroscopy (Figures S3 and S4) and ^{13}C cross-polarization magic angle spinning (CP/MAS) solid-state NMR spectroscopy (Figures S5 and S6). The FT-IR spectra of COF-524-Cu and COF-525-Cu featured characteristic C=N stretching vibrations at 1,665 and 1,656 cm^{-1} , respectively, corroborating the formation of imine bonds. The formation of imine linkages was further confirmed by ^{13}C CP/MAS solid-state NMR spectroscopy, in which the characteristic C=N imine resonance was observed at 158 ppm, which could be differentiated from the C=N double bond of the

¹Department of Chemistry and Kavli Energy Nanoscience Institute, University of California, Berkeley, Berkeley, CA 94720, USA

²Bakar Institute of Digital Materials for the Planet, Division of Computing, Data Science, and Society, University of California, Berkeley, Berkeley, CA 94720, USA

³Chemical Engineering, School for Engineering of Matter, Transport and Energy, Arizona State University, Tempe, AZ 85287, USA

⁴Center for Applied Structural Discovery, Biodesign Institute, Arizona State University, Tempe, AZ, USA

⁵Shanghai Key Laboratory of High-Resolution Electron Microscopy, School of Physical Science and Technology, ShanghaiTech University, Shanghai 201210, China

⁶Department of Mechanical Engineering, University of California, Berkeley, Berkeley, CA 94720, USA

⁷Materials Science Division, Lawrence Berkeley National Laboratory, Berkeley, CA 94720, USA

⁸Department of Materials Science & Engineering, University of California, Berkeley, Berkeley, CA 94720, USA

⁹Department of Inorganic Chemistry, Universidad de Granada, 18071 Granada, Spain

¹⁰School of Chemistry and Chemical Engineering, Frontiers Science Center for Transformative Molecules and State Key Laboratory of Metal Matrix Composites, Shanghai Jiao Tong University, Shanghai 200240, China

¹¹Lead contact

*Correspondence: yongcui@sjtu.edu.cn (Y.C.), yaghi@berkeley.edu (O.M.Y.)

<https://doi.org/10.1016/j.chempr.2023.07.015>

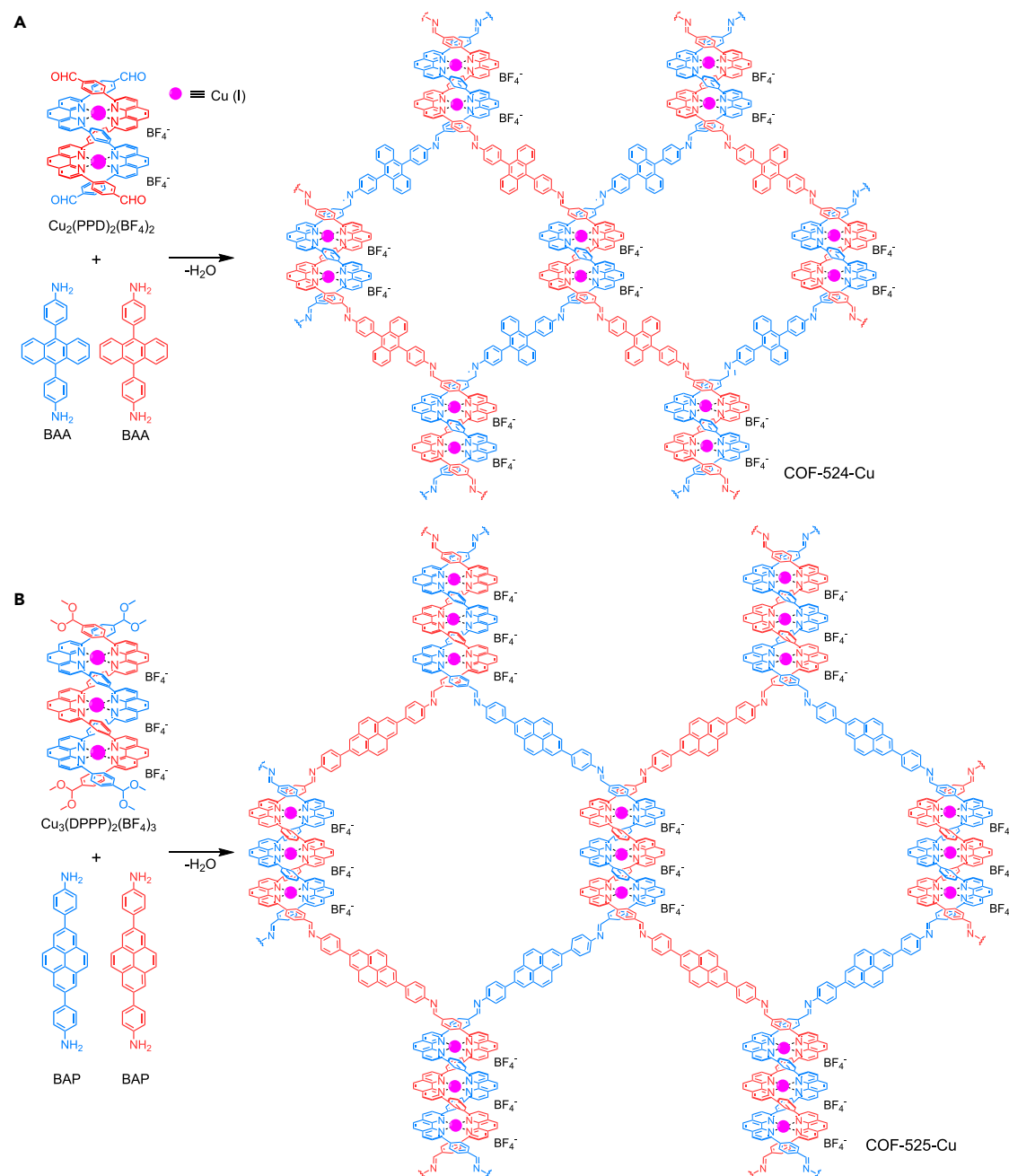


Figure 2. General strategy for the design and synthesis of woven frameworks resembling chicken-wire structures

COF-524-Cu (A) and COF-525-Cu (B) constructed from organic threads with copper(I) as a template to make 2D extended weaving structures.

phenanthroline unit located at around 152 ppm. Additionally, the disappearance of resonances above 192 ppm for COF-524-Cu, as well as 54 and 100 ppm for COF-525-Cu, demonstrates full conversion of the $\text{Cu}_2(\text{PPD})_2(\text{BF}_4)_2$ aldehyde and $\text{Cu}_3(\text{DPPP})_2(\text{BF}_4)_3$ dimethyl acetal starting material. These results support completeness of the reaction and formation of imine bonds between the building blocks to form extended framework structures. The thermal stability of both COFs studied by thermogravimetric analysis (TGA) measured under a N_2 atmosphere and the onset of the thermal decomposition of both COFs were found to be at $\sim 300^\circ\text{C}$

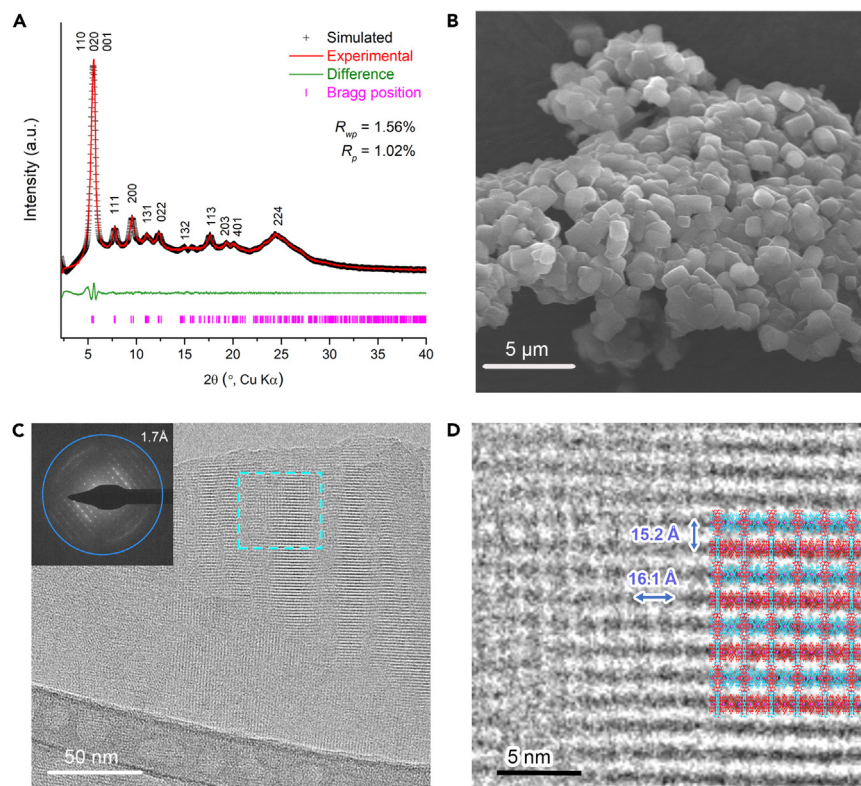


Figure 3. Structural characterization of COF-525-Cu

(A) Indexed PXRD pattern of the activated COF-525-Cu samples (red) and Pawley refinement (black) of the unit cell from the modeled structures.
(B) SEM micrograph of the COF-525-Cu crystallites indicate a single morphological phase with a homogeneous distribution of crystal sizes of $\sim 1 \mu\text{m}$.
(C) HRTEM image of COF-525-Cu. Inset: electron diffraction pattern acquired from a selected area of the crystal confirms the single crystalline nature of the particles.
(D) Magnified view of the highlighted area overlaid with a structure model showing good agreement along [100].

(Figure S7). Both COFs exhibited powder X-ray diffraction (PXRD) patterns with sharp peaks and low background that matched the predicted patterns of the simulated structures (Figures 3A and S10).

Structure determination

Scanning electron microscopy (SEM) micrographs showed a homogeneous morphology of rod-shaped crystals for COF-524-Cu and prism-shaped crystals for COF-525-Cu (Figures 3B and S8). After ultrasonication of the sample in isopropanol, individual COF crystals were dispersed on a copper sample grid for transmission electron microscopy (TEM) analysis. We collected 3D electron diffraction tomography (3D-EDT) data of COF-524-Cu by combining specimen tilt and electron-beam tilt in the range of -49.6° to $+50.6^\circ$ with a beam-tilt step of 0.3° and further processed them with an EDT-process program.^{15,16} From the acquired dataset, the 3D reciprocal lattice of COF-524-Cu was constructed and found to have unit-cell parameters of $a = 25.01 \text{ \AA}$, $b = 19.99 \text{ \AA}$, $c = 12.20 \text{ \AA}$, and $V = 6,099.4 \text{ \AA}^3$, $\alpha = \beta = \gamma = 90^\circ$ (Figure S9). From the acquired data, a structural model of COF-524-Cu was built in Materials Studio 8.0 in the orthorhombic space group $P222$. The unit-cell parameters were optimized further by Pawley refinement of the PXRD pattern to be $a = 25.84 \text{ \AA}$, $b = 20.76 \text{ \AA}$, $c = 12.87 \text{ \AA}$, and $V = 6,904.0 \text{ \AA}^3$ ($R_{wp} = 1.30\%$, $R_p = 0.97\%$). The

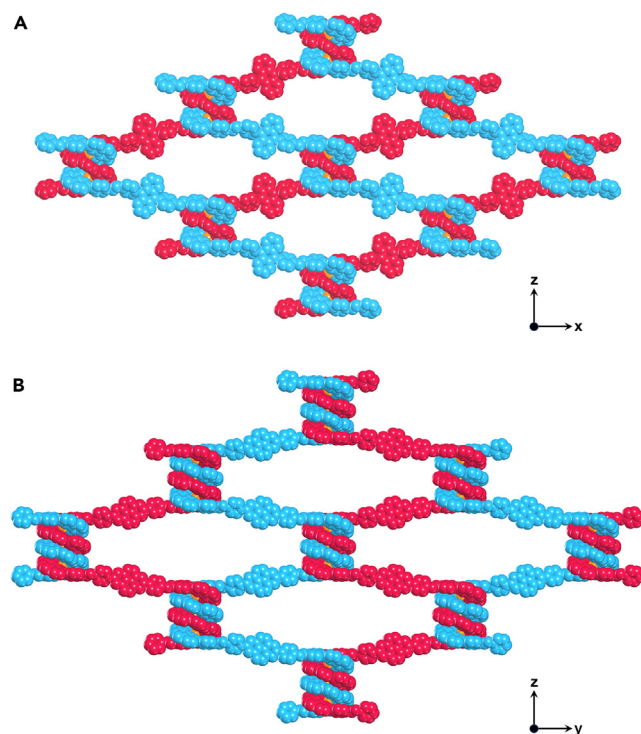


Figure 4. Modeled crystal structures of the woven COFs

(A) The diagonal blue and red linear threads are woven to form the 2D structure of COF-524-Cu. Each of the threads is periodically crossing all threads that are orthogonal to it.
(B) The 2D structure COF-525-Cu formed by the weaving of adjacent parallel zigzag threads (blue and red). Each of the threads is periodically crossing all threads that are parallel to it.
All hydrogen atoms and BF_4^- ions are omitted for clarity. Copper atoms, orange.

calculated PXRD pattern of the modeled structure was found to be in good agreement with the experimental pattern of COF-524-Cu (Figure S10).

For COF-525-Cu, we identified and analyzed a single crystal by using microcrystal electron diffraction (MicroED).^{17,18} We collected the MicroED dataset by rotating the crystal by 65° in the electron beam at a rate of 1.0° per second. We processed the diffraction dataset to 1.71 \AA by using X-ray Detector Software (XDS) to identify the unit cell parameters and space group,¹⁹ which were determined to be $C222$, $a = 18.45 \text{ \AA}$, $b = 30.68 \text{ \AA}$, $c = 15.61 \text{ \AA}$, and $V = 8,836 \text{ \AA}^3$ (Figures 3C and S12). The structural model of COF-525-Cu was constructed on the basis of this information, and the simulated PXRD pattern showed great alignment with the experimental pattern. The unit cell parameters were further optimized by Pawley refinement of the PXRD pattern to be $a = 18.45 \text{ \AA}$, $b = 31.08 \text{ \AA}$, $c = 16.00 \text{ \AA}$, and $V = 9,181 \text{ \AA}^3$ with very low discrepancy factors ($R_p = 1.02\%$, $R_{wp} = 1.56\%$; Figure 3A).

According to the refined model, COF-525-Cu crystallizes in hexagonal wire meshes by pseudo-square-planar building units $\text{Cu}_3(\text{DPPP})_2(\text{BF}_4)_3$ and linear linkers BAP connected through imine bonds. Covalently linked 1D zigzag threads propagate along the crystallographic c axis, and adjacent parallel threads are mechanically braided by triple-turn helicates at each crossing point, thus forming a chicken-wire motif with $32.0 \times 62.2 \text{ \AA}$ meshes along the crystallographic b axis (Figures 4B and S14). These 2D frameworks are two-fold interpenetrated along the b axis, such that each layer is staggered along the a axis (AB stacking), and leave enough space

for the BF_4^- counterions (Figure S14). We collected high-resolution TEM (HRTEM) images to gain further insight into the crystal structure of COF-525-Cu. The striped pattern of the lattice fringes observed in the HRTEM image shown in Figure 3D, which are separated by 16.1 and 15.2 Å, is in good agreement with the copper ions located within each crossing point.

We note that in the context of reticular chemistry, the number of turns in the crossing points directs how the threads are woven in the crystalline network. By substituting the triple-turn helicates with double-turn helicates, we were able to synthesize COF-524-Cu, which also exhibited the expected pattern of two-fold-interpenetrated chicken-wire weaving with staggered stacking (Figures 4A and S13). The average background subtraction filter (ABSF) HRTEM image of COF-524-Cu was taken along the [010] direction. The striped pattern of the lattice fringes observed in the HRTEM image shown in Figure S11, which are separated by 12.87 and 12.92 Å, is in good agreement with the structural model viewed along the [010] direction. However, unlike the motif observed in COF-525-Cu, in which the structural pattern is formed by the weaving of zigzag threads with two adjacent parallel threads, in COF-524-Cu, the two sets of diagonal linear threads propagate in an opposite direction. The diagonal blue and red linear threads are woven to form the 2D structure, and each of the threads is periodically crossing all threads that are orthogonal to it (Figure 4A). Although COF-524-Cu and -525-Cu are all composed of homochiral helicates in one crystal domain, the mixed enantiomeric isomers give rise to overall racemic woven frameworks (Figures S15 and S16).

We sought to remove the Cu ions and examine the properties of the materials before and after demetalation. Heating the COFs in a potassium cyanide (KCN) solution of *n*-butanol/water (3:1) yielded metal-free structures. Using inductively coupled plasma atomic emission spectroscopy (ICP-AES), we confirmed that 94%–97% of the Cu(I) copper ions had been removed (Table S6). The dark-brown or red color of COF-524-Cu and COF-525-Cu changed to pale yellow or gray for COF-524 and COF-525, respectively, as the demetalation proceeded (Figures S17 and S18). As expected, the crystallinity of the demetalated material decreased in comparison with that of the pristine COFs (Figures S19 and S20), but its dense structure remained unchanged, as evidenced by the N_2 adsorption tests (Figure S21). The SEM images show similar morphology and crystal sizes before and after demetalation (Figures S8 and S24). Additionally, the imine linkages were also maintained throughout the process: the characteristic FT-IR stretches at 1,665 and 1,656 cm^{-1} were consistent with those of COF-524 and COF-525, respectively (Figures S22 and S23). Furthermore, we could remetalate the material with Cu(I) ions by stirring it in a $\text{CH}_3\text{CN}/\text{CH}_2\text{Cl}_2$ solution of $\text{Cu}(\text{CH}_3\text{CN})_4\text{BF}_4$ to give back crystalline COF-524-Cu and COF-525-Cu. Although the PXRD patterns show peak broadening and loss of some diffraction features, these remetalated COFs could partially recover their crystalline structure similarly to the original as-synthesized COFs (Figures S19 and S20). In the FT-IR spectrum, the peak representing the imine $\text{C}=\text{N}$ stretch was retained, indicating that the framework is chemically stable and robust under such reaction conditions (Figures S22 and S23).

Mechanical properties

We measured the mechanical properties of the metalated and demetalated COFs by using nanoindentation. The Young's modulus values of COF-524-Cu and COF-525-Cu were 3.41 (± 0.72) and 2.38 (± 0.74) GPa, respectively, which are less rigid than the reported values for the 3D woven COF-505 and wCOF-Ag and a similar order of magnitude to other reported values of 2D COFs²⁰ or common polymers.^{8,20–23} The

hardness values of COF-524-Cu and COF-525-Cu were 124.79 (± 46.61) and 92.82 (± 33.50) MPa, respectively (Figures S25 and S26). Moreover, the demetalation process could further enhance their mechanical flexibility (2.28 [± 0.75] and 1.56 [± 0.64] GPa for COF-524 or -525, respectively) as a result of the increased degree of freedom due to the loose interactions between the threads upon the removal of copper ions.

Conclusions and outlook

We developed a new approach to achieve 2D woven COFs by installing functionalized polynuclear helicates. The pseudo-planar square geometry of the helicate linkers facilitates the creation of 2D frameworks that closely resemble chicken-wire fences while also enabling precise control over the resulting pattern type. The even and odd turn numbers of the helices directly influence the woven structures, thus allowing for the production of a new class of woven COFs through this strategy.

EXPERIMENTAL PROCEDURES

Resource availability

Lead contact

Requests for further information and resources should be directed to and will be fulfilled by the lead contact, Omar M. Yaghi (yaghi@berkeley.edu).

Materials availability

All materials generated in this study are available from the lead contact without restriction.

Data and code availability

Crystallographic data for the two crystals (tentatively assigned as right handed) reported in this article have been deposited at the Cambridge Crystallographic Data Centre under deposition numbers CCDC: 2237071 (COF-524-Cu), 2237072 (COF-525-Cu), 2238919 (model compound-1), and 2269879 (model compound-2). Copies of the data can be obtained free of charge via <https://www.ccdc.cam.ac.uk/structures/>. The datasets generated during this study are available from the lead contact without restriction.

Synthesis of COF-524-Cu

A Pyrex tube measuring 10 \times 8 mm (outside diameter [o.d.] \times inside diameter [i.d.]) was charged with Cu₂(PPD)₂(BF₄)₂ (8 mg, 0.005 mmol), BAA (3.6 mg, 0.01 mmol), 1 mL of anhydrous dioxane, and 0.4 mL of 6 M aqueous acetic acid solution. The tube was flash frozen at 77 K (liquid N₂ bath), evacuated to an internal pressure of 50 mTorr, and flame sealed. Upon sealing, the length of the tube was reduced to 13–15 cm. The reaction was heated at 120°C for 7 days, yielding a brown solid at the bottom of the tube, which was isolated by centrifugation, washed with anhydrous THF, and dried at 120°C under 50 mTorr for 12 h. This material is insoluble in water and common organic solvents such as hexanes, methanol, acetone, tetrahydrofuran, *N,N*-dimethylformamide, and dimethyl sulfoxide, indicating the formation of an extended structure. Yield: 9.7 mg, 86.3% based on Cu₂(PPD)₂(BF₄)₂. Elemental analysis results: calcd for C₂₈₀H₁₆₀B₄N₂₄F₁₆Cu₄·8H₂O: C 73.01%, H 3.85%, N 7.30%. Found: C 73.29%, H 3.79%, N 7.40%.

Synthesis of COF-525-Cu

A Pyrex tube measuring 10 \times 8 mm (o.d. \times i.d.) was charged with Cu₃(DPPP)₂(BF₄)₃ (12.2 mg, 0.005 mmol), BAP (3.8 mg, 0.01 mmol), 0.3 mL of DMA, 0.7 mL of CB, and 0.1 mL of 6 M aqueous acetic acid solution. The tube was flash frozen at 77 K (liquid N₂ bath), evacuated to an internal pressure of 50 mTorr, and flame sealed. Upon

sealing, the length of the tube was reduced to 13–15 cm. The reaction was heated at 120°C for 3 days, yielding a brown solid at the bottom of the tube, which was isolated by centrifugation, washed with anhydrous THF, and dried at 120°C under 50 mTorr for 12 h. This material is insoluble in water and common organic solvents such as hexanes, methanol, acetone, tetrahydrofuran, *N,N*-dimethylformamide, and dimethyl sulfoxide, indicating the formation of an extended structure. Yield: 9.7 mg, 86.3% based on $\text{Cu}_3(\text{DPPP})_2(\text{BF}_4)_3$. Elemental analysis results: calcd for $\text{C}_{360}\text{H}_{208}\text{B}_6\text{N}_{32}\text{F}_{24}\text{Cu}_6 \cdot 8\text{H}_2\text{O}$: C 71.73%, H 3.75%, N 7.44%. Found: C 71.87%, H 3.72%, N 7.51%.

SUPPLEMENTAL INFORMATION

Supplemental information can be found online at <https://doi.org/10.1016/j.chempr.2023.07.015>.

ACKNOWLEDGMENTS

This research was supported by King Abdulaziz City for Science and Technology (KACST) as part of a joint KACST-UC Berkeley Center of Excellence for Nanomaterials for Clean Energy Applications and by the Defense Advanced Research Projects Agency (DARPA) under contract HR001-119-S-0048. We acknowledge the College of Chemistry Nuclear Magnetic Resonance Facility for resource instruments at UC Berkeley, which are partially supported by NIH S10OD024998, and staff assistance from Dr. Hasan Celik. This research used resources of beamline 12.2.1 at the Advanced Light Source, which is a DOE Office of Science User Facility under contract no. DE-AC02-4105CH11231. X.H. acknowledges the support of the National Natural Science Foundation of China (22005188). We would like to acknowledge the use of the Titan Krios at the Eyring Materials Center at Arizona State University and the funding of this instrument by NSF MRI 1531991. J.A.R.N. is grateful to the Spanish Ministry of Universities for a Salvador Madariaga-Fulbright grant (PRX21/00093). The authors thank Prof. George Lisensky (Beloit College) and Haoze Wang for their helpful discussions.

AUTHOR CONTRIBUTIONS

X.H. and O.M.Y. conceived the idea and led the project. X.H. and T.M. conducted the synthesis and crystal growth. B.L.N., X.Y., and Y.Z. carried out electron diffraction study and structure refinement. P.K., J.K., and R.O.R. performed the nanoindentation test. K.W. and Z.R. contributed to material characterization. X.H. and O.M.Y. wrote the manuscript with help from S.E.N. and J.A.R.N. All authors discussed and revised the manuscript.

DECLARATION OF INTERESTS

The authors declare no competing interests.

Received: April 19, 2023

Revised: June 29, 2023

Accepted: July 24, 2023

Published: August 18, 2023

REFERENCES

1. Yaghi, O., Kalmutzki, M., and Diercks, C. (2019). Introduction to Reticular Chemistry: Metal–Organic Frameworks and Covalent Organic Frameworks (Wiley-VCH Verlag GmbH). <https://doi.org/10.1002/9783527821099>.
2. Lewandowska, U., Zajaczkowski, W., Corra, S., Tanabe, J., Borrmann, R., Benetti, E.M., Stappert, S., Watanabe, K., Ochs, N.A.K., Schaeublin, R., et al. (2017). A triaxial supramolecular weave. *Nat. Chem.* 9, 1068–1072. <https://doi.org/10.1038/nchem.2823>.
3. August, D.P., Dryfe, R.A.W., Haigh, S.J., Kent, P.R.C., Leigh, D.A., Lemonnier, J.F., Li, Z., Murny, C.A., Palmer, L.I., Song, Y., et al. (2020). Self-assembly of a layered two-dimensional molecularly woven fabric. *Nature* 588, 429–435. <https://doi.org/10.1038/s41586-020-3019-9>.
4. Ciengshin, T., Sha, R., and Seeman, N.C. (2011). Automatic molecular weaving prototyped by using single-stranded DNA. *Angew. Chem. Int.*

- Ed. 50, 4419–4422. <https://doi.org/10.1002/anie.201007685>.
5. Liu, Y., Ma, Y., Yang, J., Diercks, C.S., Tamura, N., Jin, F., and Yaghi, O.M. (2018). Molecular weaving of covalent organic frameworks for adaptive guest inclusion. *J. Am. Chem. Soc.* 140, 16015–16019. <https://doi.org/10.1021/jacs.8b08949>.
6. Zhao, Y., Guo, L., Gándara, F., Ma, Y., Liu, Z., Zhu, C., Lyu, H., Trickett, C.A., Kapustin, E.A., Terasaki, O., et al. (2017). A synthetic route for crystals of woven structures, uniform nanocrystals, and thin films of imine covalent organic frameworks. *J. Am. Chem. Soc.* 139, 13166–13172. <https://doi.org/10.1021/jacs.7b07457>.
7. Liu, Y., Diercks, C.S., Ma, Y., Lyu, H., Zhu, C., Alshimmri, S.A., Alshihri, S., and Yaghi, O.M. (2019). 3D covalent organic frameworks of interlocking 1D square ribbons. *J. Am. Chem. Soc.* 141, 677–683. <https://doi.org/10.1021/jacs.8b12177>.
8. Liu, Y., Ma, Y., Zhao, Y., Sun, X., Gándara, F., Furukawa, H., Liu, Z., Zhu, H., Zhu, C., Suenaga, K., et al. (2016). Weaving of organic threads into a crystalline covalent organic framework. *Science* 351, 365–369. <https://doi.org/10.1126/science.aad4011>.
9. Kramer, R., Lehn, J.M., and Marquis-Rigault, A. (1993). Self-recognition in helicate self-assembly: spontaneous formation of helical metal complexes from mixtures of ligands and metal ions. *Proc. Natl. Acad. Sci. USA* 90, 5394–5398. <https://doi.org/10.1073/pnas.90.12.5394>.
10. Lehn, J. (2009). Towards complex matter: supramolecular chemistry and self-organization. *Eur. Rev.* 17, 263–280. <https://doi.org/10.1017/S1062798709000805>.
11. Piguett, C., Bernardinelli, G., and Hopfgartner, G. (1997). Helicates as versatile supramolecular complexes. *Chem. Rev.* 97, 2005–2062. <https://doi.org/10.1021/cr960053s>.
12. Ayme, J.F., Beves, J.E., Campbell, C.J., and Leigh, D.A. (2013). Template synthesis of molecular knots. *Chem. Soc. Rev.* 42, 1700–1712. <https://doi.org/10.1039/c2cs35229j>.
13. Dietrich-Buchecker, C., Rapenne, G., Sauvage, J., De Cian, A., and Fischer, J. (1999). A dicopper(II) trefoil knot with m-phenylene bridges between the ligand subunits: synthesis, resolution, and absolute configuration. *Chem. Eur. J.* 5, 1432–1439. [https://doi.org/10.1002/\(SICI\)1521-3765\(19990503\)5:5<1432::AID-CHEM1432>3.0.CO;2-C](https://doi.org/10.1002/(SICI)1521-3765(19990503)5:5<1432::AID-CHEM1432>3.0.CO;2-C).
14. Dietrich-Buchecker, C., and Sauvage, J. (1999). Lithium templated synthesis of catenanes: efficient synthesis of doubly interlocked [2]-catenanes. *Chem. Commun.* 7, 615–616. <https://doi.org/10.1039/a809885i>.
15. Gemmi, M., and Oleynikov, P. (2013). Scanning reciprocal space for solving unknown structures: energy filtered diffraction tomography and rotation diffraction tomography methods. *Z. für Krist. Cryst. Mater.* 228, 51–58. <https://doi.org/10.1524/zkri.2013.1559>.
16. Zhang, Y.B., Su, J., Furukawa, H., Yun, Y., Gándara, F., Duong, A., Zou, X., and Yaghi, O.M. (2013). Single-crystal structure of a covalent organic framework. *J. Am. Chem. Soc.* 135, 16336–16339. <https://doi.org/10.1021/ja409033p>.
17. Nannenga, B.L. (2020). MicroED methodology and development. *Struct. Dyn.* 7, 014304. <https://doi.org/10.1063/1.5128226>.
18. Nannenga, B.L., and Gonen, T. (2019). The cryo-EM method microcrystal electron diffraction (MicroED). *Nat. Methods* 16, 369–379. <https://doi.org/10.1038/s41592-019-0395-x>.
19. Kabsch, W. (2010). XDS. *Acta Crystallogr. D Biol. Crystallogr.* 66, 125–132. <https://doi.org/10.1107/S0907444909047337>.
20. Fang, Q., Sui, C., Wang, C., Zhai, T., Zhang, J., Liang, J., Guo, H., Sandoz-Rosado, E., and Lou, J. (2021). Strong and flaw-insensitive two-dimensional covalent organic frameworks. *Matter* 4, 1017–1028. <https://doi.org/10.1016/j.matt.2021.01.001>.
21. Xu, H.S., Luo, Y., Li, X., See, P.Z., Chen, Z., Ma, T., Liang, L., Leng, K., Abdelwahab, I., Wang, L., et al. (2020). Single crystal of a one-dimensional metallo-covalent organic framework. *Nat. Commun.* 11, 1434. <https://doi.org/10.1038/s41467-020-15281-1>.
22. Tan, J.C., and Cheetham, A.K. (2011). Mechanical properties of hybrid inorganic-organic framework materials: establishing fundamental structure–property relationships. *Chem. Soc. Rev.* 40, 1059–1080. <https://doi.org/10.1039/c0cs00163e>.
23. Zeng, Y., Gordiichuk, P., Ichihara, T., Zhang, G., Sandoz-Rosado, E., Wetzel, E.D., Tresback, J., Yang, J., Kozawa, D., Yang, Z., et al. (2022). Irreversible synthesis of an ultrastrong two-dimensional polymeric material. *Nature* 602, 91–95. <https://doi.org/10.1038/s41586-021-04296-3>.